# Transient perturbative nonlinear responses of plasmonic materials

Mikko J. Huttunen, Jussi Kelavuori, and Marco Ornigotti
*Photonics Laboratory, Physics Unit, Tampere University, FI-33014 Tampere, Finland*

(Received 8 May 2020; accepted 1 December 2020; published 18 December 2020)

Recent investigations on optical nonlinearities of plasmonic materials suggest their responses may be even beyond the usual perturbative description. To better understand these surprisingly strong responses, we develop here a simple but general approach to describe the nonlinear optical response of plasmonic materials up to *n*th perturbation order. We apply the approach to understand spectral broadening occurring in resonant metasurfaces and investigate the enhancement of multiharmonic generation from multiply resonant metasurfaces, predicting an over $1\times10^6$-fold enhancement of higher harmonics.

DOI: 10.1103/PhysRevA.102.063525

## I. INTRODUCTION

Photonic metamaterials, i.e., artificial materials that enable subwavelength length scale control of light, play a key role in modern nanophotonics [1,2]. Besides the study of the linear optical responses of metamaterials, a growing interest has emerged in the recent years to understand also their nonlinear responses [3–7], as they are essential in many different applications including frequency conversion, high- and multiharmonic generation (MHG), ultrashort pulse generation, and frequency combs [8,9]. Spectral broadening and supercontinuum generation (SCG) are particularly interesting nonlinear phenomena that are utilized to make spectrally broad and coherent light sources [10], which have found numerous applications for example in gas sensing [11], generation of few-cycle pulses [12,13], optical metrology [14], spectroscopy [15,16], and optical coherence tomography [17]. Consequently, these two nonlinear phenomena are of considerable scientific and technological interest.

Spectral broadening and SCG occur ubiquitously in solids, liquids, and gases [18–23]. Unfortunately, the intrinsic material nonlinearities giving rise to these phenomena are very weak, making it necessary to use strong excitation pulses from amplified laser systems with peak intensities of the order of $10^{14}$ W/cm$^2$ to exploit those nonlinear effects. Nonlinear optical fibers, for example, provide a relatively flexible platform that can be also utilized with moderate peak intensities [10]. However, their big disadvantage is the requirement for long interaction lengths, which makes them incompatible with the small footprint typical of nanophotonic devices.

Integrated photonic supercontinuum sources, on the other hand, are characterized by small footprint and compatibility with mass production, representing an ideal platform for the realization of on-chip SCG [14,24]. The recent demonstrations of SCG from plasmonic nanoparticles and metasurfaces, in particular, have raised the interest to further investigate their properties, in particular the out-of-equilibrium dynamics of conduction electrons occurring in such systems, as they are responsible for both SCG and spectral broadening [25–27]. Many of the experiments have been performed using only moderate peak intensities ($10^{10}$–$10^{11}$ W/cm$^2$), prompting the investigation of the possible origins of the responses, because conventional theory predicts the necessity to use order-of-magnitude higher intensities to realize efficient SCG from such thin materials [27].

Moreover, because the complex dynamics of conduction electrons in plasmonic materials dictate their optical properties [25], it seems natural to assume that the same dynamics are pivotal also in SCG occurring in such systems. To this aim, the hydrodynamic model has recently reemerged as a powerful tool to understand the conduction electron dynamics [28–30], and has also been used to propose that nonlocal and nonperturbative effects occurring in plasmonic materials could play a major role in the surprisingly strong SCG [27,30]. However, it is not yet clear whether other effects could also participate in the process.

In this paper, we investigate the transient nonlinear responses of plasmonic systems motivated by the fact that modern experiments are often performed using ultrashort laser pulses. We extend the simple anharmonic oscillator model, commonly used to describe nonlinear responses, by taking into account the transient response of the system and by generalizing the treatment to include up to $n$ perturbation orders. We show that considerable spectral broadening of ultrashort pulses may take place in resonant plasmonic systems, such as in metasurfaces. We also predict that dramatic six to seven order-of-magnitude enhancement of higher-harmonic processes up to sixth harmonic could occur in plasmonic structures exhibiting multiple resonances.

Our paper is organized as follows: In Sec. II we use the Green's-function approach to extend the usual anharmonic oscillator model to include the transient dynamics up to *n*th perturbation order. In Sec. III we discuss how accounting for the transient response of the system could result in a significant broadening of the incident ultrafast pulse. We also discuss how the transient contributions into the light-matter interaction could result in a significant enhancement of the MHG

 

process in multiresonant plasmonic structures. In Sec. IV, we draw the conclusions.

## II. THEORY

We start our analysis by considering the classical anharmonic oscillator model and seek to describe the time-varying displacement of the conduction electron $\tilde{x}(t)$. We assume the electron to be forced into motion by an incident field

$$\tilde{E}(t) = \frac{1}{\sqrt{2\pi}} \int_{\Delta\omega} E(\omega') e^{-i\omega' t}\, d\omega', \tag{1}$$

where the Fourier integral extends over the incident pulse frequencies $\Delta\omega$ centered at the fundamental frequency $\omega$. We further assume $\tilde{E}$ to be strong enough, so that the electron oscillation becomes noticeably anharmonic, while we take $\tilde{E}$ to be weak enough to allow describing the anharmonic motion perturbatively. In this case, the forced oscillation of the electron displacement can be described using the classical anharmonic oscillator model [31]

$$\ddot{\tilde{x}} + 2\gamma\dot{\tilde{x}} + \omega_0^2\tilde{x} + a\tilde{x}^2 = -e\tilde{E}(t)/m, \tag{2}$$

where $\gamma$ is the damping constant, $\omega_0$ is the resonance frequency of the oscillator, $e$ is the electric charge, $m$ is the effective mass of the electron, and $a$ is a parameter describing the anharmonicity of the oscillator. The tilde and overdot notations denote time-varying quantities and their time derivatives, respectively. We also note that the above anharmonic oscillator model applies for noncentrosymmetric materials where quadratic nonlinearities are allowed [31]. Generalization of the treatment to centrosymmetric materials is straightforward but long, given therefore as the Appendix. Although no analytical solutions of Eq. (2) are available, in the case of weak nonlinearities ($a\tilde{x} \ll \omega_0^2$), an approximate perturbative solution of form

$$\tilde{x}(t) = \tilde{x}_1(t) + \tilde{x}_2(t) + \tilde{x}_3(t) + \cdots + \tilde{x}_n(t) \tag{3}$$

is commonly solved up to the first few orders in terms of its steady-state solution [31]. Here, we extend the conventional treatment to include the transient response of the oscillator and by finding a general solution taking into account perturbative corrections up to $n$th order. This allows us to calculate the perturbative behavior of the anharmonic oscillator for arbitrary input profiles $\tilde{E}(t)$.

Substituting the ansatz above into Eq. (2) and equating the terms of the same perturbative order, we get the following set of coupled differential equations, for the various perturbation orders:

$$\ddot{\tilde{x}}_1 + 2\gamma\dot{\tilde{x}}_1 + \omega_0^2\tilde{x}_1 = -e\tilde{E}(t)/m, \tag{4a}$$
$$\ddot{\tilde{x}}_2 + 2\gamma\dot{\tilde{x}}_2 + \omega_0^2\tilde{x}_2 = -a\tilde{x}_1^2, \tag{4b}$$
$$\ddot{\tilde{x}}_3 + 2\gamma\dot{\tilde{x}}_3 + \omega_0^2\tilde{x}_3 = -2a\tilde{x}_1\tilde{x}_2, \tag{4c}$$
$$\vdots$$
$$\ddot{\tilde{x}}_n + 2\gamma\dot{\tilde{x}}_n + \omega_0^2\tilde{x}_n = -a\sum_{|\alpha|=2}\binom{2}{\alpha}\tilde{x}^\alpha. \tag{4d}$$

The right-hand side of the $n$th equation follows from the multinomial theorem, and takes use of the multi-indices $\alpha = (\alpha_1, \alpha_2, \ldots, \alpha_n)$ and $\tilde{x}^\alpha = \tilde{x}_1^{\alpha_1}\tilde{x}_2^{\alpha_2}\ldots\tilde{x}_n^{\alpha_n}$. Note that $\tilde{x}_3$ can be seen to arise from cascaded nonlinear processes, where light generated by the second-order correction term ($\tilde{x}_2$) gives rise to higher-order terms via process of sum-frequency generation. Similarly, the higher-order terms can be seen to arise from cascaded processes of lower order.

The complete linear response, i.e., the solution of Eq. (4a), can be written as a convolution of the Green's function $\tilde{G}$ of the unperturbed oscillator and the incident field $\tilde{E}$ [32]:

$$\tilde{x}_1(t) = -\frac{e}{m}\int_{-\infty}^{\infty}\tilde{G}(t-t')\tilde{E}(t')\,dt' = -\frac{e}{m}\tilde{G}\circledast\tilde{E}. \tag{5}$$

In the last equality we have introduced $\circledast$ as a shorthand to indicate the convolution operation. The time-domain Green's function of an underdamped oscillator is [32]

$$\tilde{G}(t) = \frac{e^{-\gamma t}}{\omega_{\rm tr}}\sin(\omega_{\rm tr}t)\Theta(t), \tag{6}$$

where $\omega_{\rm tr} = \sqrt{\omega_0^2 - \gamma^2}$ is the natural frequency of the oscillator and $\Theta(t)$ is the step function imposed due to causality of the system. Note that Eq. (5) contains an important result: while the motion of an electron described by Eq. (5) will, at equilibrium, oscillate following the driving field $\tilde{E}(t)$, on a timescale of the order of $\tau = \gamma^{-1}$, the electron oscillates also at its natural frequency $\omega_{\rm tr}$, rather than only following the impinging field. If this transient timescale, which for bulk gold and silver, for example, is around 10 and 30 fs, respectively [33], is comparable with the characteristic timescale of the driving pulse, efficient coupling between the transient and driven electron dynamics will take place.

The solution for the second- and third-order correction terms $\tilde{x}_2$ and $\tilde{x}_3$ can then be found by solving Eqs. (4b) and (4c) with the aid of the first-order solution. To do that, it is convenient to work in the frequency domain, where the convolution can be regarded as a simple multiplication, allowing us to rewrite Eq. (5) as

$$\hat{x}_1(\omega) = -\frac{e}{m}\hat{G}(\omega)\hat{E}(\omega), \tag{7}$$

where the hat notation indicates that the variable is described in the frequency domain. The frequency-domain Green's function of the underdamped oscillator $\hat{G}(\omega)$ is explicitly given as

$$\hat{G}(\omega) = \frac{A_0}{\omega_{\rm tr}}\left(\frac{1}{\gamma + i(\omega - \omega_{\rm tr})} - \frac{1}{\gamma + i(\omega + \omega_{\rm tr})}\right), \tag{8}$$

where the scaling of the spectral amplitude $A_0$ is dictated by the investigated structure. Using Eq. (7) and the result above, the solutions of Eqs. (4b)–(4d) can be then written in the following compact form:

$$\hat{x}_2(\omega) = -a\,\hat{G}(\omega)[\hat{x}_1(\omega)\circledast\hat{x}_1(\omega)], \tag{9a}$$
$$\hat{x}_3(\omega) = -2a\,\hat{G}(\omega)[\hat{x}_1(\omega)\circledast\hat{x}_2(\omega)], \tag{9b}$$
$$\vdots$$
$$\hat{x}_n(\omega) = -a\,\hat{G}(\omega)\sum_{|\alpha|=2}\binom{2}{\alpha}\hat{x}^\alpha(\omega). \tag{9c}$$

Here, the $n$th-order solution is concisely written using multi-index notation $\hat{x}^{\alpha} = \hat{x}_1^{\alpha_1} \circledast \hat{x}_2^{\alpha_2} \circledast \ldots \circledast \hat{x}_n^{\alpha_n}$. Note that because convolution in the frequency domain results in a sum between the various frequencies involved in the process, $\hat{x}_2(\omega)$ contains terms that oscillate, in addition to the expected frequency $2\omega$, also at frequencies $2\omega_{\mathrm{tr}}$, and $\omega + \omega_{\mathrm{tr}}$, corresponding, respectively, to the second-harmonic generation centered at the transient frequency, and sum-frequency generation involving the driving frequency and the transient frequency. Similarly, $\hat{x}_3(\omega)$ will contain terms oscillating, in addition to the expected $3\omega$, also at $3\omega_{\mathrm{tr}}$, $2\omega + \omega_{\mathrm{tr}}$, and $2\omega_{\mathrm{tr}} + \omega$.

Equations (9a)–(9c) are the main result of our paper, and allow us a convenient way to find the general solution for the driven anharmonic oscillator system governed by Eq. (2) up to the $n$th perturbative order. This general solution includes the possible transient contributions to the overall response, which may be important either when the driving fields are very short pulses (≈fs) or when the system exhibits dynamics occurring at similar/longer time scales.

Taking into account the transient dynamics of the conduction electrons in plasmonic systems gives rise to the generation of new frequencies and modulation of existing frequency components associated with the incident pulse. Interestingly, we see that the characteristic transient frequency of the system $\omega_{\mathrm{tr}}$ dictates the occurrence of the nonlinear processes allowing means to engineer them. For example, one could control the spectral broadening of an incident pulse by designing a system where the center frequency of the incident pulse and the transient frequency $\omega_{\mathrm{tr}}$ coincide, where the strongest spectral broadening is expected to occur near $\omega_{\mathrm{tr}}$. This spectral broadening mechanism is interesting because the frequency components retain their phase coherence potentially being useful also for ultrashort pulse generation [8,34].

## III. RESULTS AND DISCUSSION

To validate our findings, we first calculate the emission spectrum of a metasurface consisting of identical plasmonic gold nanoparticles, by using the perturbative solution to Eq. (3) as found above. The nanoparticles are taken to exhibit a localized plasmon resonance, peaking near 1.54 eV and associated with the relaxation time $\tau = 10$ fs similar to bulk gold [33]. The nonlinear coefficient $a$ was taken to be $20\,\mathrm{m^{-1}\,s^{-2}}$, resulting in calculated SHG efficiencies that agree with earlier experiments on gold nanoparticle arrays [35].

We start our analysis by taking an incident pulse with a Gaussian temporal profile with a full width at half maximum of 100 fs, centered at $\lambda = 805$ nm (1.54 eV), and investigate the spectral broadening of the incident field upon interaction. The peak intensity of the incident pulse is assumed to be $20\,\mathrm{TW/cm^2}$, which can be readily achieved using a beam from an amplified system, such as a 1-kHz amplifier with 15-mW average power, focused to a spot with a radius of $20\,\mu$m. A representative calculated emission spectrum obtained from the metasurface defined above is shown in Fig. 1, where the spectral broadening of the incident pump field (red solid curve) is clearly visible. The calculations were repeated while varying the number of included perturbative terms $n = 5$, 10, and 15. For each calculation, the validity of the perturbation expansion was carefully checked by calculating the amplitude of $a\tilde{x}$. In all cases, $a\tilde{x} < 3.4\times10^{12}\ \mathrm{s^{-2}} \ll \omega_0^2$, validating the perturbative approach. Surprisingly high perturbative terms ($n > 10$) were found to still visibly affect the predicted spectral broadening. This demonstrates the power of the introduced approach, which allows these contributions to be included with ease. Overall, the result shown in Fig. 1 suggests that resonant metasurfaces could be used also for spectral broadening of ultrashort pulses. The advantages of metasurfaces compared to traditional materials include compact size, wavelength tunability, and the possibility to engineer the wavefront of interacting free-space beams [36,37]. In addition, metasurfaces are free of phase-matching considerations, that arise from material dispersion in conventional nonlinear bulk materials [6].

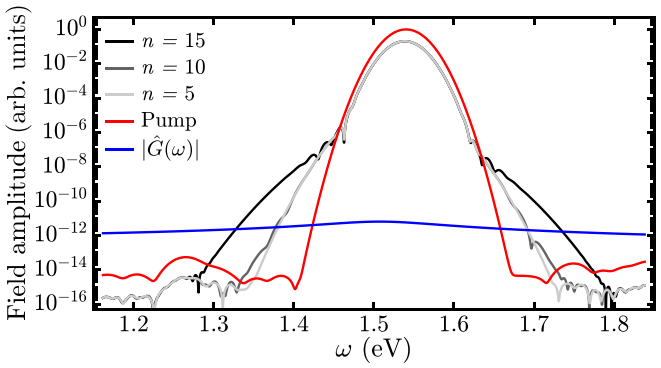


FIG. 1. Calculated emission spectrum showing spectral broadening as a function of included perturbation terms $n$. The input pump (red curve) is centered at 805 nm (1.54 eV), and a single material resonance ($\tau = 10$ fs) is taken to coincide with the pump wavelength. The blue curve acts as a guide to the eye and visualizes the spectral profile of the Green's function associated with the metasurface.

As a second demonstration of the introduced approach, we investigate MHG in plasmonic metasurfaces. It has been recently realized that collective responses of periodic nanostructures can support narrow resonances [38–40]. The decay times of these narrow resonances can be considerably longer than those of bulk metals. In addition, the possibility to fabricate metasurfaces supporting multiple resonances has also been recently demonstrated [41,42]. Here, we are interested to understand how the emission spectrum and process of MHG could be engineered by utilizing the above-mentioned plasmonic metasurfaces exhibiting multiple narrow resonances.

First, we consider the metasurface and incident pulse as described above except for the assumed peak intensity. Here, we use a lower peak intensity of $100\,\mathrm{GW/cm^2}$. Such peak intensity can already be achieved using a 20-mW mean power output beam from a 1-MHz repetition rate oscillator, now focusing the beam into a spot with a radius of $10\,\mu$m. Such excitation conditions result in mean power below $0.07\,\mathrm{mW}/\mu\mathrm{m}^2$, which is considerably lower than $1\text{–}10\,\mathrm{mW}/\mu\mathrm{m}^2$ powers that have been reported to result in heating-induced damage of plasmonic nanomaterials [43]. In the calculations, the first ten perturbative terms are taken into account ($n = 10$). Again, the validity of the perturbation expansion was checked by calculating the amplitude of

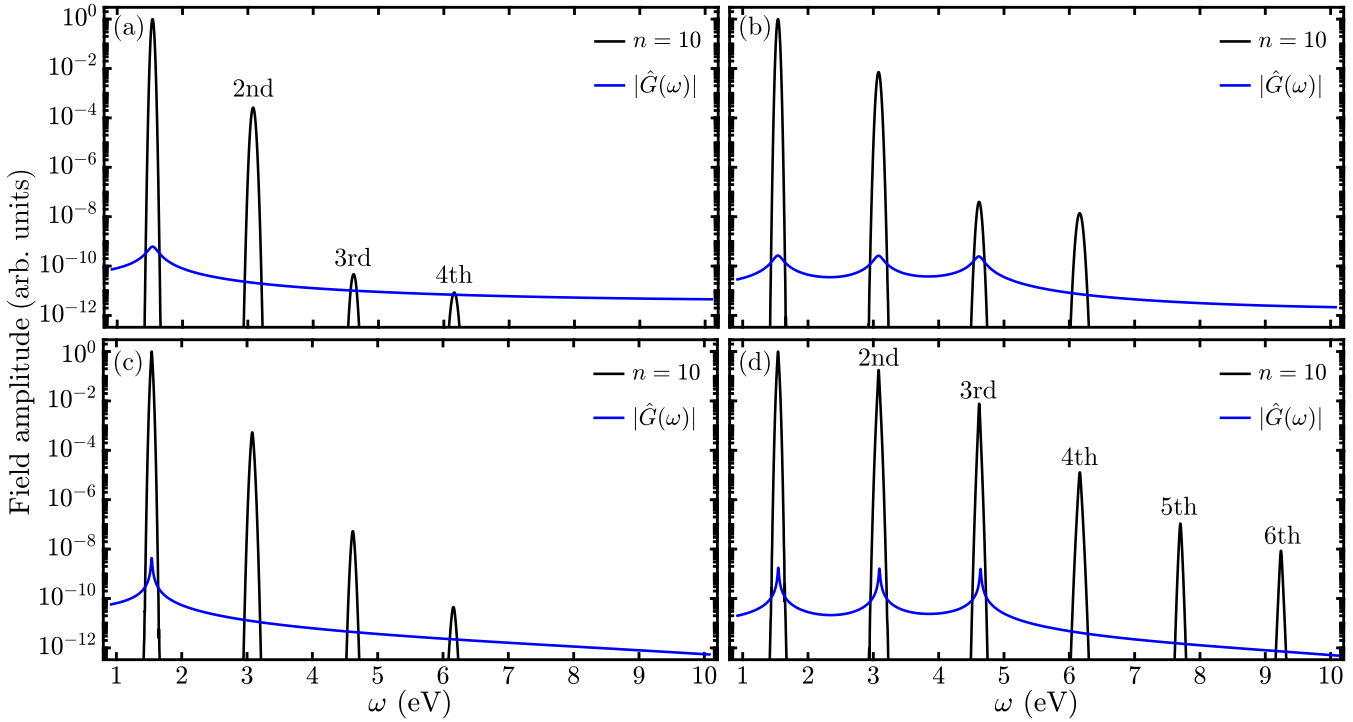


FIG. 2. Calculated emission spectrum (for $n = 10$) using a pump beam centered at 1.54 eV. Blue curves act as guides to the eye and visualize the Green's functions associated with the metasurfaces. Emission spectra for singly resonant (a) and multiresonant (b) metasurfaces associated with resonances exhibiting relaxation times of $\tau = 10$ fs. MHG up to the fourth harmonic is visible. Emission spectra for singly resonant (c) and multiresonant (d) metasurfaces with $\tau = 100$ fs. (d) MHG up to the sixth harmonic is clearly visible.

$a\tilde{x}$, which was found in all calculations to be smaller than $8.2\times10^{10}\,\mathrm{s}^{-2}$, validating the approach. The calculated emission spectrum is shown in Fig. 2(a), demonstrating MHG. Then we study a multiresonant metasurface that exhibits material resonances at frequencies of 1.54, 3.08, and 4.62 eV, which coincide with the fundamental, second-, and third-harmonic peaks of the incident pulse. The relaxation times of these resonances are taken to be the same as above ($\tau = 10$ fs). As these resonances occur at the harmonics of the incident pulse frequency (1.54 eV), their presence is expected to enhance MHG. This is also seen in the calculated emission spectrum shown in Fig. 2(b), where most notably the field amplitude of the fourth-harmonic peak is increased 1560-fold compared to the singly resonant metasurface [Fig. 2(a)].

We then investigate singly and multiply resonant metasurfaces that exhibit resonances with longer relaxation times ($\tau = 100$ fs) than considered above. As mentioned in Sec. II, 100-fs-long pulses used to excite the metasurfaces are expected to couple almost optimally to such resonances. We also note that such metasurfaces could potentially be realized by utilizing Fabry-Pérot resonances and collective responses occurring in metasurfaces [41,42]. The calculated emission spectra for these singly and multiply resonant metasurfaces are shown in Figs. 2(c) and 2(d), respectively. Comparing the calculated emission spectra of singly resonant metasurfaces [Figs. 2(a) and 2(c)], we see that the narrower resonance results in a 7700-fold (40-fold) enhancement of third-harmonic generation (fourth-harmonic generation).

It is even more interesting to compare the emission spectra of the singly resonant metasurface against the multiresonant case with narrow resonances [Figs. 2(a) and 2(d)]. In this case, the field enhancements are calculated to be $3.94\times10^6$ ($10.36\times10^6$) for the third-harmonic (fourth-harmonic) peak. We also note for the case of the multiresonant metasurface that even the fifth-harmonic and sixth-harmonic peaks are now clearly visible. Together these results prompt the investigation of how such multiresonant metasurfaces could be designed and realized [41,42].

Next, we discuss the origin of the higher-order processes of spectral broadening and MHG, as it might seem surprising that the anharmonic oscillator model [Eq. (2)], exhibiting only a quadratic nonlinearity, predicts their occurrence. However, their origin is understood by considering cascaded nonlinear processes, where the lower-order nonlinear processes give rise to effective higher-order nonlinear processes [44–48]. Here, at the beginning of the light-matter interaction, the quadratic nonlinearity gives rise to second-order processes and associated new frequency components [Eq. (9a)], that will later on act as seeds in further quadratic nonlinear interactions [Eq. (9b)]. These and subsequent cascaded second-order processes will then effectively manifest as higher-order processes [Eq. (9c)]. Therefore, we see that by using the introduced approach such cascaded higher-order processes can be taken into account simply by including higher-order perturbative terms. This is interesting because our approach allows simple and intuitive means to understand and even engineer the occurrence of higher-order processes in metasurfaces.

Then, we consider the asymptotic behavior of the model by taking an increasingly long relaxation time $\tau$ (i.e., vanishingly small damping term $\gamma$). In this case, the transient responses

no longer quickly decay, suggesting that they remain non-negligible even under continuous-wave illumination. Despite vanishingly small $\gamma$ being strictly nonphysical, we note that recent experimental and numerical investigations on collective responses of metal nanoparticle arrays, known as surface lattice resonances, suggest that systems associated with quite long relaxation times (≈ps) can be fabricated [38,39,49]. Furthermore, even though the relaxation times of plasmonic excitations can be controlled to a degree by changing the temperature of the system [50], we believe it is considerably easier to design structures such as studied here by engineering the relaxation times by controlling the radiative losses of the system [49].

Last, we consider the validity of the perturbative description for the studied resonant and multiresonant metasurfaces. In all the cases studied here, the assumption of weak nonlinearities ($a\tilde{x} \ll \omega_0^2$) was strictly valid and the perturbative description adequate. However, we note that for metasurfaces supporting long-lasting plasmon excitations saturation effects arising from the complex population dynamics of the associated conduction electrons might start playing a role. In such cases, the introduced model that only considers the dynamics of a single conduction electron will obviously be inadequate. However, despite these limitations we think that the introduced model will be a highly useful tool for understanding the main driving parameters of studied multiresonant metasurfaces.

## IV. CONCLUSIONS

We have investigated the nonlinear optical responses of plasmonic materials by extending the anharmonic oscillator model, commonly used to describe nonlinear responses, by taking into account also the transient response of the system and by finding a general solution including up to $n$ perturbative orders. The approach allows us to better understand the nonlinear responses of these materials and provides means to engineer their responses for applications, such as for spectral broadening or frequency conversion. Our results suggest that considerable spectral broadening of ultrashort pulses may occur in metasurfaces due to the transient response of the system. We also predict that higher-harmonic processes, namely, the sixth-harmonic generation, could be enhanced over a $1\times10^6$-fold by utilizing multiply resonant plasmonic structures.

## ACKNOWLEDGMENTS

We thank Ksenia Dolgaleva for her valuable feedback and comments. We acknowledge the support of the Academy of Finland (Grant No. 308596) and the Flagship of Photonics Research and Innovation (PREIN) funded by the Academy of Finland (Grant No. 320165).

## APPENDIX

For completeness, here we generalize concisely the introduced treatment to centrosymmetric materials. Because of symmetry considerations, the quadratic anharmonicity term vanishes, resulting in the cubic anharmonic oscillator model [31]:

$$\ddot{\tilde{x}} + 2\gamma\dot{\tilde{x}} + \omega_0^2\tilde{x} + b\tilde{x}^3 = -e\tilde{E}(t)/m, \tag{A1}$$

where all the variables have been already defined in the main text except for the parameter $b$ that is the cubic anharmonicity of the system. Again, in the case of weak nonlinearities ($b\tilde{x}^2 \ll \omega_0^2$), an approximate perturbative steady-state solution now of the form

$$\tilde{x}(t) = \tilde{x}_1(t) + \tilde{x}_3(t) + \tilde{x}_5(t) + \cdots + \tilde{x}_n(t) \tag{A2}$$

can be found [31]. Here, we extend the conventional treatment by finding a general perturbative solution to Eq. (A1) by taking into account perturbative corrections up to the $n$th order. This allows us to also calculate the perturbative behavior of the cubic anharmonic oscillator for arbitrary input profiles $\tilde{E}(t)$.

Substituting the ansatz of Eq. (A2) into Eq. (A1) and equating the terms of the same perturbative order, we get the following set of coupled differential equations, for the various perturbation orders:

$$\ddot{\tilde{x}}_1 + 2\gamma\dot{\tilde{x}}_1 + \omega_0^2\tilde{x}_1 = -e\tilde{E}(t)/m, \tag{A3a}$$
$$\ddot{\tilde{x}}_3 + 2\gamma\dot{\tilde{x}}_3 + \omega_0^2\tilde{x}_3 = -b\tilde{x}_1^3, \tag{A3b}$$
$$\ddot{\tilde{x}}_5 + 2\gamma\dot{\tilde{x}}_5 + \omega_0^2\tilde{x}_5 = -3b\tilde{x}_1^2\tilde{x}_3, \tag{A3c}$$
$$\ddot{\tilde{x}}_7 + 2\gamma\dot{\tilde{x}}_7 + \omega_0^2\tilde{x}_7 = -3b(\tilde{x}_1^2\tilde{x}_5 + \tilde{x}_3^2\tilde{x}_1), \tag{A3d}$$
$$\vdots$$
$$\ddot{\tilde{x}}_n + 2\gamma\dot{\tilde{x}}_n + \omega_0^2\tilde{x}_n = -b\sum_{|\alpha|=3}\binom{3}{\alpha}\tilde{x}^\alpha. \tag{A3e}$$

The concisely written equation for the general $n$th-order term again makes use of the multi-index notation.

Transforming the above equations into the frequency domain and by using Eq. (7), the solutions for Eqs. (A3b)–(A3e) can be then written compactly as

$$\hat{x}_3(\omega) = -a\,\hat{G}(\omega)[\hat{x}_1(\omega) \circledast \hat{x}_1(\omega) \circledast \hat{x}_1(\omega)], \tag{A4a}$$
$$\hat{x}_5(\omega) = -3b\,\hat{G}(\omega)[\hat{x}_1(\omega) \circledast \hat{x}_1(\omega) \circledast \hat{x}_3(\omega)], \tag{A4b}$$
$$\hat{x}_7(\omega) = -3b\,\hat{G}(\omega)[\hat{x}_1(\omega) \circledast \hat{x}_1(\omega) \circledast \hat{x}_5(\omega) + \hat{x}_3(\omega) \circledast \hat{x}_3(\omega) \circledast \hat{x}_1(\omega)], \tag{A4c}$$
$$\vdots$$
$$\hat{x}_n(\omega) = -b\,\hat{G}(\omega)\sum_{|\alpha|=3}\binom{3}{\alpha}\hat{x}^\alpha(\omega). \tag{A4d}$$

Again, multi-index notation $\hat{x}^\alpha = \hat{x}_1^{\alpha_1} \circledast \hat{x}_2^{\alpha_2} \circledast \ldots \circledast \hat{x}_n^{\alpha_n}$ is used. Looking at the above terms, it is clear that the found perturbative solution reproduces the known experimental result that such cubic (i.e., centrosymmetric) media result in MHG spectra, solely consisting of the odd harmonics of the pump. However, our approach does provide insights and design criteria to develop novel materials, such as nonlinear metamaterials or two-dimensional materials [51,52], for nonlinear processes of interest, such as for MHG. For example, looking at the above solution we see that by designing the nonlinear material to exhibit resonances at frequencies $3\omega$ and/or $5\omega$, the overall efficiency to generate the seventh harmonic could be enhanced. Perhaps more importantly, in addition to

enhancing the efficiency of the process, such resonance engineering could be utilized to control the phase of the generated harmonic component [53–55]. Such intuition cannot be easily formed by resorting to purely numerical approaches.


[1] A. Alù, M. G. Silveirinha, A. Salandrino, and N. Engheta, Phys. Rev. B **75**, 155410 (2007).
[2] C. M. Soukoulis and M. Wegener, Nat. Photon. **5**, 523 (2011).
[3] M. Kauranen and A. V. Zayats, Nat. Photon. **6**, 737 (2012).
[4] M. Lapine, I. V. Shadrivov, and Y. S. Kivshar, Rev. Mod. Phys. **86**, 1093 (2014).
[5] J. Butet, P. F. Brevet, and O. J. Martin, ACS Nano **9**, 10545 (2015).
[6] G. Li, S. Zhang, and T. Zentgraf, Nat. Rev. Mater. **2**, 17010 (2017).
[7] E. Rahimi and R. Gordon, Adv. Opt. Mater. **6**, 1 (2018).
[8] T. Brabec and F. Krausz, Rev. Mod. Phys. **72**, 545 (2000).
[9] T. J. Kippenberg, R. Holzwarth, and S. A. Diddams, Science **332**, 555 (2011).
[10] J. M. Dudley, G. Genty, and S. Coen, Rev. Mod. Phys. **78**, 1135 (2006).
[11] J. M. Langridge, T. Laurila, R. S. Watt, R. L. Jones, C. F. Kaminski, and J. Hult, Opt. Express **16**, 10178 (2008).
[12] J. M. Dudley and S. Coen, Opt. Express **12**, 2423 (2004).
[13] M. A. Foster, A. L. Gaeta, Q. Cao, and R. Trebino, Opt. Express **13**, 6848 (2005).
[14] A. R. Johnson, A. S. Mayer, A. Klenner, K. Luke, E. S. Lamb, M. R. E. Lamont, C. Joshi, Y. Okawachi, F. W. Wise, M. Lipson, U. Keller, and A. L. Gaeta, Opt. Lett. **40**, 5117 (2015).
[15] P. Domachuk, N. A. Wolchover, M. Cronin-Golomb, A. Wang, A. K. George, C. M. B. Cordeiro, J. C. Knight, and F. G. Omenetto, Opt. Express **16**, 7161 (2008).
[16] C. R. Petersen, U. Møller, I. Kubat, B. Zhou, S. Dupont, J. Ramsay, T. Benson, S. Sujecki, N. Abdel-Moneim, Z. Tang, D. Furniss, A. Seddon, and O. Bang, Nat. Photon. **8**, 830 (2014).
[17] B. Schenkel, J. Biegert, and U. Keller, Opt. Lett. **28**, 1987 (2003).
[18] R. R. Alfano and S. L. Shapiro, Phys. Rev. Lett. **24**, 592 (1970).
[19] P. B. Corkum, C. Rolland, and T. Srinivasan-Rao, Phys. Rev. Lett. **57**, 2268 (1986).
[20] F. A. Ilkov, L. S. Ilkova, and S. L. Chin, Opt. Lett. **18**, 681 (1993).
[21] M. Kolesik, G. Katona, J. V. Moloney, and E. M. Wright, Phys. Rev. Lett. **91**, 043905 (2003).
[22] P.-a. Champert, V. Couderc, P. Leproux, S. Février, V. Tombelaine, L. Labonté, P. Roy, and C. Froehly, Opt. Express **12**, 4366 (2004).
[23] F. Silva, D. R. Austin, A. Thai, M. Baudisch, M. Hemmer, D. Faccio, A. Couairon, and J. Biegert, Nat. Commun. **3**, 807 (2012).
[24] D. Y. Oh, D. Sell, H. Lee, K. Y. Yang, S. A. Diddams, and K. J. Vahala, Opt. Lett. **39**, 1046 (2014).
[25] P. Muehlschegel, H. Eisler, O. J. F. Martin, B. Hecht, P. Mu, and D. W. Pohl, Science **308**, 1607 (2005).
[26] P. Biagioni, D. Brida, J. S. Huang, J. Kern, L. Duò, B. Hecht, M. Finazzi, and G. Cerullo, Nano Lett. **12**, 2941 (2012).
[27] J. Chen, A. Krasavin, P. Ginzburg, A. V. Zayats, T. Pullerits, and K. J. Karki, ACS Photon. **5**, 1927 (2018).
[28] J. E. Sipe, V. C. Y. So, M. Fukui, and G. I. Stegeman, Phys. Rev. B **21**, 4389 (1980).
[29] M. Scalora, M. A. Vincenti, D. De Ceglia, V. Roppo, M. Centini, N. Akozbek, and M. J. Bloemer, Phys. Rev. A **82**, 043828 (2010).
[30] A. V. Krasavin, P. Ginzburg, G. A. Wurtz, and A. V. Zayats, Nat. Commun. **7**, 1 (2016).
[31] R. W. Boyd, in *Nonlinear Optics*, 2nd ed. (Academic Press, New York, 2017), p. 578.
[32] F. W. Byron and R. W. Fuller, *Mathematics of Classical and Quantum Physics* (Dover Publications, New York, 1992).
[33] P. B. Johnson, P. B. Johnson, and R. W. Christy, Phys. Rev. B **6**, 4370 (1972).
[34] G. Steinmeyer, D. H. Sutter, L. Gallmann, N. Matuschek, and U. Keller, Science **286**, 1507 (1999).
[35] R. Czaplicki, A. Kiviniemi, M. J. Huttunen, X. Zang, T. Stolt, I. Vartiainen, J. Butet, M. Kuittinen, O. J. F. Martin, and M. Kauranen, Nano Lett. **18**, 7709 (2018).
[36] W. Ye, F. Zeuner, X. Li, B. Reineke, S. He, C. W. Qiu, J. Liu, Y. Wang, S. Zhang, and T. Zentgraf, Nat. Commun. **7**, 11930 (2016).
[37] F. Walter, G. Li, C. Meier, S. Zhang, and T. Zentgraf, Nano Lett. **17**, 3171 (2017).
[38] B. Auguié and W. L. Barnes, Phys. Rev. Lett. **101**, 143902 (2008).
[39] M. J. Huttunen, K. Dolgaleva, P. Törmä, and R. W. Boyd, Opt. Express **24**, 28279 (2016).
[40] V. G. Kravets, A. V. Kabashin, W. L. Barnes, and A. N. Grigorenko, Chem. Rev. **118**, 5912 (2018).
[41] M. J. Huttunen, O. Reshef, T. Stolt, K. Dolgaleva, R. W. Boyd, and M. Kauranen, J. Opt. Soc. Am. B **36**, E30 (2019).
[42] O. Reshef, M. Saad-Bin-Alam, M. J. Huttunen, G. Carlow, T. Sullivan, J.-M. Ménard, K. Dolgaleva, and R. W. Boyd, Nano Lett. **19**, 6429 (2019).
[43] J. Beermann, R. L. Eriksen, T. Holmgaard, K. Pedersen, and S. I. Bozhevolnyi, Sci. Rep. **4**, 6904 (2014).
[44] G. Assanto, G. I. Stegeman, E. VanStryland, and M. Sheik-Bahae, IEEE J. Quantum Electron. **31**, 673 (1995).
[45] X. Mu, X. Gu, M. V. Makarov, Y. J. Ding, J. Wang, J. Wei, and Y. Liu, Opt. Lett. **25**, 117 (2000).
[46] L. Misoguti, S. Backus, C. G. Durfee, R. Bartels, M. M. Murnane, and H. C. Kapteyn, Phys. Rev. Lett. **87**, 013601 (2001).
[47] K. Dolgaleva, H. Shin, and R. W. Boyd, Phys. Rev. Lett. **103**, 113902 (2009).
[48] M. Celebrano, A. Locatelli, L. Ghirardini, G. Pellegrini, P. Biagioni, A. Zilli, X. Wu, S. Grossmann, L. Carletti, C. De Angelis, L. Duò, B. Hecht, and M. Finazzi, Nano Lett. **19**, 7013 (2019).
[49] M. S. Bin-Alam, O. Reshef, Y. Mamchur, M. Z. Alam, G. Carlow, J. Upham, B. T. Sullivan, J.-M. Ménard, M. J.

Huttunen, R. W. Boyd, and K. Dolgaleva, arXiv:2004.05202v2 (2020).

[50] J. S. G. Bouillard, W. Dickson, D. P. O'Connor, G. A. Wurtz, and A. V. Zayats, Nano Lett. **12**, 1561 (2012).

[51] H. Liu, Y. Li, Y. S. You, S. Ghimire, T. F. Heinz, and D. A. Reis, Nat. Phys. **13**, 262 (2017).

[52] A. Autere, H. Jussila, Y. Dai, Y. Wang, H. Lipsanen, and Z. Sun, Adv. Mater. **30**, 1705963 (2018).

[53] P. Balcou, A. L'Huillier, and D. Escande, Phys. Rev. A **53**, 3456 (1996).

[54] T. Popmintchev, M. C. Chen, A. Bahabad, M. Gerrity, P. Sidorenko, O. Cohen, S. Backus, X. Zhang, G. Taft, I. P. Christov, M. M. Murnane, and H. C. Kapteyn, Proc. Natl. Acad. Sci. USA **106**, 10516 (2009).

[55] T. Stolt, J. Kim, A. Vesala, R. Czaplicki, M. Kauranen, J. Rho, and P. Genevet, arXiv:2006.06988 (2020).